

See discussions, stats, and author profiles for this publication at: <https://www.researchgate.net/publication/229892750>

# Characteristics and OSL minimum ages of relict fluvial deposits near Sossus Vlei, Tsauchab River, Namibia, and a regional climate record for the last 30 ka

Article in *Journal of Quaternary Science* · May 2006

DOI: 10.1002/jqs.977

CITATIONS

34

READS

209

3 authors, including:



**Pradeep Srivastava**

Wadia Institute of Himalayan Geology

106 PUBLICATIONS 1,906 CITATIONS

[SEE PROFILE](#)



**Eugene Marais**

Gobabeb Research and Training Centre

56 PUBLICATIONS 961 CITATIONS

[SEE PROFILE](#)

Some of the authors of this publication are also working on these related projects:



A taxonomic and phylogenetic revision of the genus *Ptenopus* (Reptilia: Gekkonidae) [View project](#)



Late Quaternary evolution of the Alaknanda valley in the vicinity of North Almora Thrust, [View project](#)

# Characteristics and OSL minimum ages of relict fluvial deposits near Sossus Vlei, Tsauchab River, Namibia, and a regional climate record for the last 30 ka

GEORGE A. BROOK,<sup>1\*</sup> PRADEEP SRIVASTAVA<sup>1†</sup> and EUGENE MARAIS<sup>2</sup>

<sup>1</sup> Department of Geography, University of Georgia, Athens, GA, USA

<sup>2</sup> National Museum of Namibia, Windhoek, Namibia

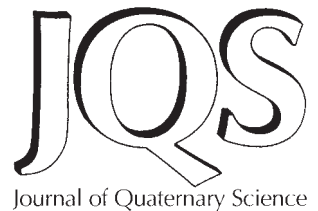
Brook, G. A., Srivastava, P. and Marais, E. 2006. Characteristics and OSL minimum ages of relict fluvial deposits near Sossus Vlei, Tsauchab River, Namibia, and a regional climate record for the last 30 ka. *J. Quaternary Sci.*, Vol. 21 pp. 347–362. ISSN 0267–8179.

Received 9 May 2005; Revised 18 August 2005; Accepted 15 September 2005

**ABSTRACT:** The present end-point of the Tsauchab River is at Sossus Vlei, 30 km into the Namib Sand Sea. Interdune deposits in three depressions west and southwest of the vlei include channel and interdune lithofacies associations but no deposits typical of river end-points or of groundwater seepage into interdune areas. The two lithofacies associations show that the Tsauchab River extended further into the sand sea in the past. It had a well-developed channel and a higher flow than today that caused flooding of adjacent interdune areas.

OSL 4-mm aliquot minimum ages indicate that the Tsauchab River reached 2–3 km beyond its present end-point at ca. 25 ka and ca. 9–7 ka, and that the river was more active from 0.9–0.3 ka. The eastward migration of the river end-point since ca. 7 ka suggests a reduction in flood magnitude accompanied by the gradual invasion of the Sossus Vlei area by dunes. The regional data indicate an additional wet interval at ca. 15 ka that is so far not recorded in the Sossus area. Copyright © 2006 John Wiley & Sons, Ltd.

**KEYWORDS:** interdune deposits; luminescence dating; climate change; Tsauchab River; Namibia.



## Introduction

Active and relict sand seas can provide important data about Quaternary climate change. The age of inactive dunes is an indication of past dune activity and a more arid climate (e.g. Stokes *et al.*, 1997; Thomas and Shaw, 2002) while interdune sediments, sometimes including fluvial deposits, may preserve evidence of wetter climate intervals (e.g. Lancaster, 1984, 1989; Teller *et al.*, 1990; Thomas *et al.*, 2003). The area covered by interdune sediments in modern sand seas can be significant, averaging 50% in the Namib Sand Sea (Lancaster and Teller, 1988). Shaw *et al.* (1992) have dated freshwater shells, calcified reeds, and freshwater carbonates in interdune areas of the Kalahari Desert to show that the Xaudum and Okwa rivers in northwest Botswana were much more active 17.5–14.5 ka.

The potential of fluvial deposits within the Namib Sand Sea to provide information on past wetter phases of climate has long been recognised (e.g. Lancaster, 1984; Heine, 1998). However, because of inaccessibility there have been relatively few studies of these deposits and none that has made extensive use of OSL dating.

Studies of the Tsondeb River (Fig. 1(A)) show fluvial and lacustrine deposits and traces of former stream channels to within 20 km of the Atlantic Ocean over a distance of 70 km west of the present end-point of the river at Tsondeb Vlei ('vlei' is the Dutch word for marsh but it is also used to refer to seasonally inundated pans and end-points of rivers), itself 30 km into the Namib Sand Sea (Vogel and Visser, 1981; Lancaster, 1984; Ward, 1987; Deacon and Lancaster, 1988). These deposits indicate a stream with much higher competence and capacity than today. Calibrated radiocarbon ages of calcified roots and freshwater mollusc shells show that the river reached Narabeb 35–23.5 ka and that by 17.2–15.8 ka its terminus had retreated eastward to a point 5–10 km west of Tsondeb Vlei. Vlei silts at Tsondeb Vlei also suggest increased river flow ca. 9.9–9.5 ka (Vogel and Visser, 1981; Lancaster, 1984; Teller and Lancaster, 1986; Deacon and Lancaster, 1988). Since ca. 16 ka several 50–100 m high dunes have blocked the course of the Tsondeb River so that the terminal playa has retreated eastwards to its present location. The large dune-free area of the Tsondeb Flats and the disturbance of the main S–N trending linear dunes to the west suggest that the Tsondeb River may have formed a barrier to northward extension of the Namib Sand Sea until after ca. 20 ka (Teller and Lancaster, 1986; Lancaster 1989).

About 70 km south of the Tsondeb the Tsauchab River currently ends at Sossus Vlei. Calibrated radiocarbon ages for

\* Correspondence to: George A. Brook, Department of Geography, University of Georgia, Athens, GA 30602, USA. E-mail: gabrook@uga.edu

† Current address: Wadia Institute of Himalayan Geology, 33 GMS Road, Dehradun—248001, India.

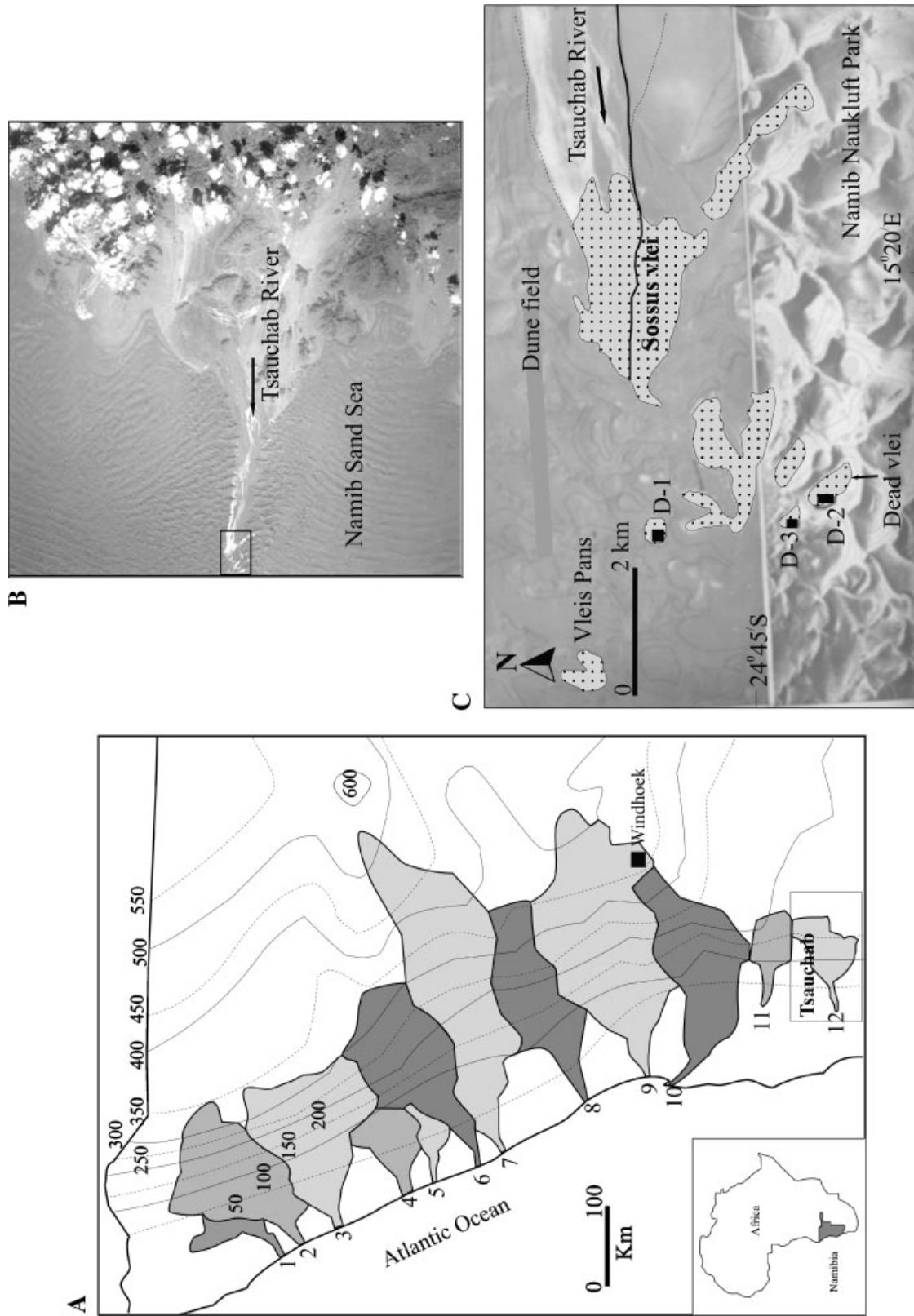


**Figure 1** (A) Map showing the westerly flowing rivers of Namibia and the location of the Tsauchab River catchment. Rainfall isohyets (in mm) are shown in broken and continuous lines (after Jacobson *et al.*, 1995). Drainage basins are: 1, Khumib; 2, Hoarusib; 3, Hoanib; 4, Uniab; 5, Koigab; 6, Huab; 7, Ugab; 8, Omaruru; 9, Swakop; 10, Kuiseb; 11, Tsondab; 12, Tsauchab. (B) Satellite image of the Tsauchab River catchment showing the present end-point of the river at Sossus Vlei. (C) Detailed map of the Sossus Vlei area showing Dead Vlei and depressions D-1 and D-3 (modified from South West Africa 1:50 000 topographic map 2415CB)

vlei silts at Sossus Vlei suggest increased flow to the playa 29–23 and 11–10 ka, with slightly increased flow at 0.7 ka (Vogel and Visser, 1981; Heine, 1998). In addition, Vogel (2003) has studied the ages of dead trees at Dead Vlei, near Sossus Vlei but separated from it by a large dune. These suggest wetter conditions 0.8–0.6 ka followed by a period of drought that killed the trees.

In this paper we describe the lithofacies composition, OSL age, and palaeoenvironmental implications of sediments in three interdune areas to the west and southwest of Sossus Vlei and isolated from it by large dunes. Based on results presented here and on previous research (e.g. Roberts *et al.*, 1999; Wallinga, 2002; Srivastava *et al.*, 2006) we have used 4-mm aliquot minimum ages for our OSL chronology. The resulting palaeoenvironmental data are viewed alongside other reliably dated climate records and a summary model for the region is proposed.

## Study area

### General background

The Namib Sand Sea covers an area of ca. 34 000 km<sup>2</sup> along the coast of Namibia. It extends for almost 400 km north of the Orange River near Luderitz along the South Atlantic coastal plain to Walvis Bay, and inland for 100–150 km. It is bounded in the east by the western escarpment of the southern African plateau and to the north by the Kuiseb River valley. Mean annual rainfall ranges from  $\leq 15$  mm on the coast to 80–100 mm near the escarpment. A number of ephemeral rivers drain towards the coast from the uplands lying beyond the escarpment (Fig. 1). The Kuiseb and rivers to the north reach the Atlantic during years of high rainfall. South of the Kuiseb rivers such as the Tsondab and the Tsauchab have small catchments that do not extend beyond the eastern margin of the desert. These rivers never reach the coast and like rivers further south they terminate in playas within the Namib Sand Sea (Fig. 1).

The focus of this study is the 4000-km<sup>2</sup> Tsauchab River catchment bordered by the Naukluft Mountains to the north, the foothills of the western escarpment to the east and the Zaris Mountains to the south. Although the catchment is entirely within an area receiving  $<150$  mm annual rainfall, the river penetrates more than 45 km into the Namib Sand Sea before terminating at Sossus Vlei, a playa (Fig. 1(B)). East of Sossus Vlei the Tsauchab valley floor is more than 3 km wide and flanked on both sides by massive dunes. The channel is incised 1–2 m into calcrete-cemented fluvial and aeolian deposits. The Namib dunes are among the highest in the world and at Sossus Vlei they crest 300–360 m above the Tsauchab River (Lancaster and Teller, 1988).

A layer of light grey silt covers the surface of Sossus Vlei and there are deep desiccation cracks in the centre of the pan. A number of very large *Acacia erioloba* trees grow around the margin, especially in the south. On three sides massive dunes border the pan (Fig. 1(C)). During most years the Tsauchab River does not reach Sossus Vlei and a new end-point is being created upstream by a thick sand body with small barchanoid dunes and vegetated sand hummocks. However, occasional floods triggered by exceptional rainfall along the western escarpment still penetrate to Sossus Vlei leaving it inundated for several weeks, as occurred for example in 1986, 1990, 1997 and 2000. To the SE, SW and W of Sossus Vlei there are a series of elongate and oval pans. Relict fluvial and pan

deposits exposed in the floors of these depressions are evidence that in the past the Tsauchab River penetrated further into the Sand Sea than it does today (Fig. 1(C)).

### Study sites

This study examines sediments exposed in the floors of three interdune depressions (D-1 to D-3) separated from Sossus Vlei by dunes up to about 50 m high. The interdune areas are dominated by fluvial sediments interspersed with aeolian deposits.

Depression 1 (D-1) is about 2 km west of the westernmost tongue of Sossus Vlei and is separated from it by a high W–E trending dune ridge (Fig. 1(C)). In the deepest part of the depression deflation has exposed rounded fluvial gravels deposited along a former river channel (Fig. 2). According to Vogel (2003) similar deposits extend to the southwest and north for a considerable distance into the region of massive linear dunes.

Southwest of Sossus Vlei is a series of pans including three oval-shaped depressions covered by a layer of grey silt about 20–80 cm thick. These are separated from each other and from Sossus Vlei by SW–NE trending linear dune ridges 10–20 m high. The largest of the oval-shaped pans is Dead Vlei (D-2), named for the large number of dead *Acacia erioloba* trees within the pan (Fig. 3). A closed erosional gully along the western margin of Dead Vlei has exposed ca. 3 m of the sediment sequence in the vlei. Some smaller *A. erioloba* trees still grow in the erosional depression indicating that at times moisture seeps into the pan from the surrounding dunes. We studied sediments exposed by gully erosion and also nearby silt and sand hummocks above the pan surface. These hummocks, as well as thin, horizontally bedded silt layers draped over the basal part of a high dune, indicate that at times the water level in this pan must have been considerably higher than the present surface.

The third interdune depression examined (D-3) is immediately NW of Dead Vlei and separated from it only by a low sand ridge. The gully along the western margin of Dead Vlei formerly discharged into this depression but was blocked and transformed into a small closed depression by development of the dune that now separates it from Dead Vlei. Sediments in D-3 have been eroded by water and wind, and remnants typically have been streamlined by wind to form yardangs a few to several metres long and a few metres high. In contrast to the flat pan surfaces of Sossus and Dead Vlei, the floor of D-3 is irregular with deep gullies and steep-sided yardang-shaped sediment residuals (Fig. 4).

Deposits in the floors of the three depressions are archives of past fluvial activity in the region near the present end-point of the Tsauchab River and of past climatic conditions in the Namib Desert. In this paper we examine the stratigraphic characteristics of sediments exposed in these interdune depressions, and discuss their age and palaeoenvironmental significance.

### Sediment characteristics

Based on physical sedimentary structure, degree of bioturbation, grain size, and geometry of sedimentary units, various lithofacies were identified in the sediments exposed in the floors of Depressions 1–3. These are described below and are shown schematically in Fig. 5.

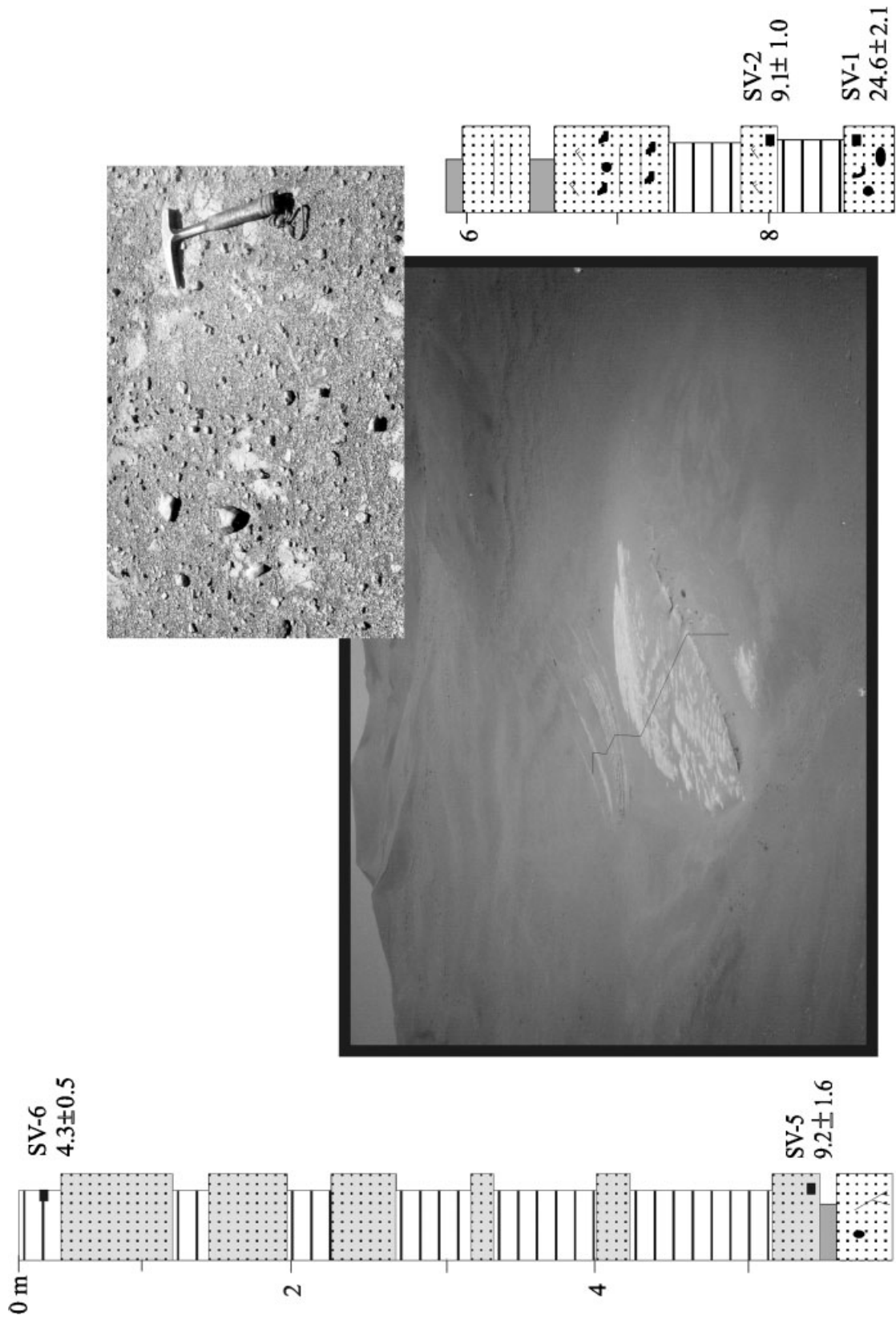


**Figure 2** Geomorphology, sediment stratigraphy, and age of depression D-1. Inset shows rounded gravels at the base of the sequence. The solid black line in the photograph of the depression mirrors changes in relief. Lithofacies shading patterns are shown in Fig. 5

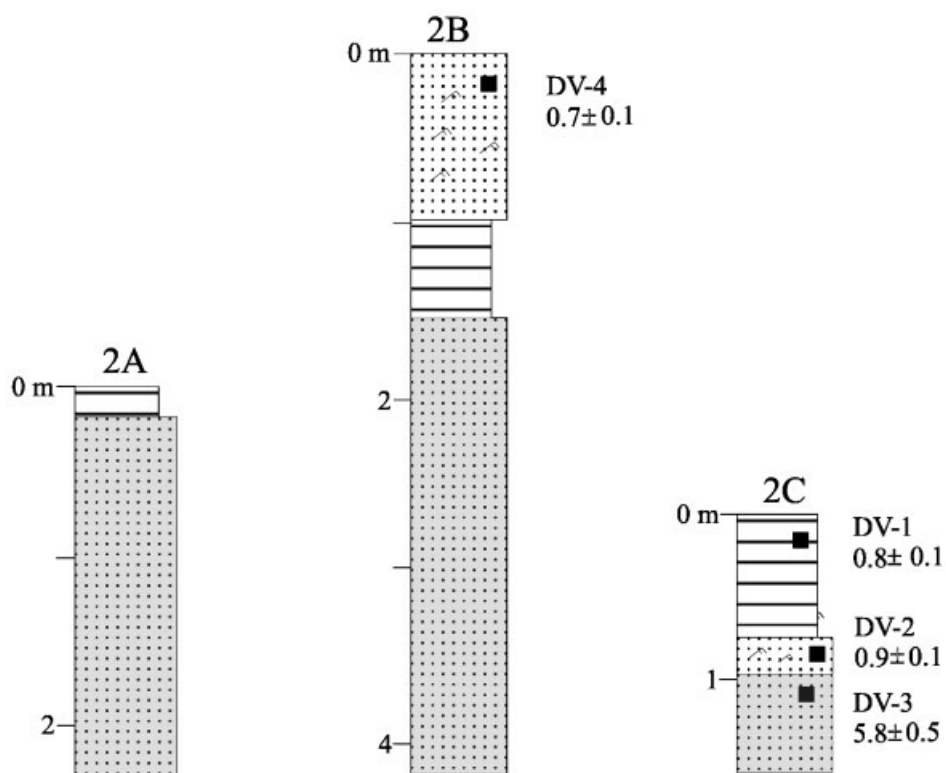


**Figure 3** Silt-covered surface of Dead Vlei (depression D-2) showing dead trees and stratigraphy and ages of sediments in Sections 2A–2C. Lithofacies shading patterns are shown in Fig. 5

### Individual lithofacies

#### Well-sorted medium sand

This is red, well-sorted, cross-stratified medium quartz sand deficient in mica, with individual lamina 2–3 mm thick. It is 0.6–2.2 m thick and overlain by a thin layer of silt. This aeolian dune deposit is well developed in Section 2C at Dead Vlei (Fig. 3). The dip of the strata indicates deposition by a S–SW palaeowind similar to the dominant wind today (Lancaster, 1982).

#### Medium sand with mud balls

This lithofacies is a reddish-brown medium sand, 0.2–1.0 m thick, generally with an erosional base and little physical structure (Fig. 5). There are only occasional ripple laminations and moderate bioturbation. Mud balls, clay curls and gravels 2–12 cm in diameter are common. In places the unit contains only clay curls in a medium sand matrix with ripple laminations. It is the diagnostic facies of the basal part of the sediment sequence examined in D-1 (Fig. 2). The unit records the fluvial reworking of aeolian sand. The clay curls and mud balls are

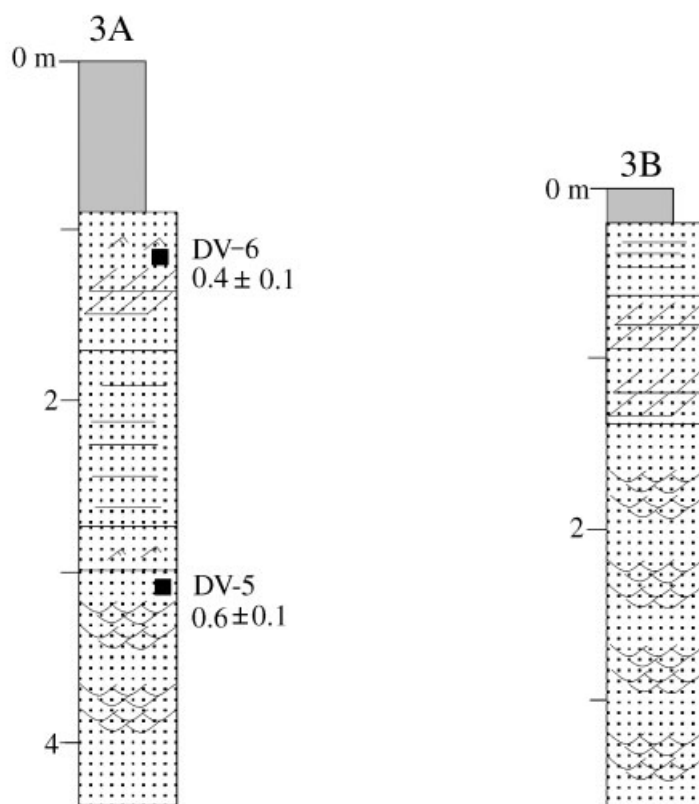


**Figure 4** Wind-eroded fluvial sediments on the floor of depression D-3 and stratigraphy and ages of sediments in Sections 3A and 3B. Lithofacies shading patterns are shown in Fig. 5

reworked clayey deposits laid down in shallow pools or interdune areas during earlier floods. Gravels indicate high-energy flood events; units without mud balls and gravels indicate low-energy floods.

#### Ripple-laminated fine sand

Units of this lithofacies consist of 0.2–0.6 m thick, red, ripple-laminated fine sand that is moderately bioturbated

and lensoid in lateral geometry. This facies generally overlies dune deposits and is followed by an alternating sand and silt facies. It often contains ellipsoidal mud clasts, up to 6.5 cm in diameter, towards the base. This lithofacies is a shallow channel deposit within the dune area. A modern analogue is described by Svendsen *et al.* (2002) who studied Hoanib River flood deposits in interdune areas of the Skeleton Coast in the northern Namib. Channels are formed in interdune areas when excess river flow is diverted laterally between dunes during high floods (Krapf *et al.*, 2003; Stanistreet and Stollhofen, 2002).

## Interdune Facies Association

## Channel Facies Association

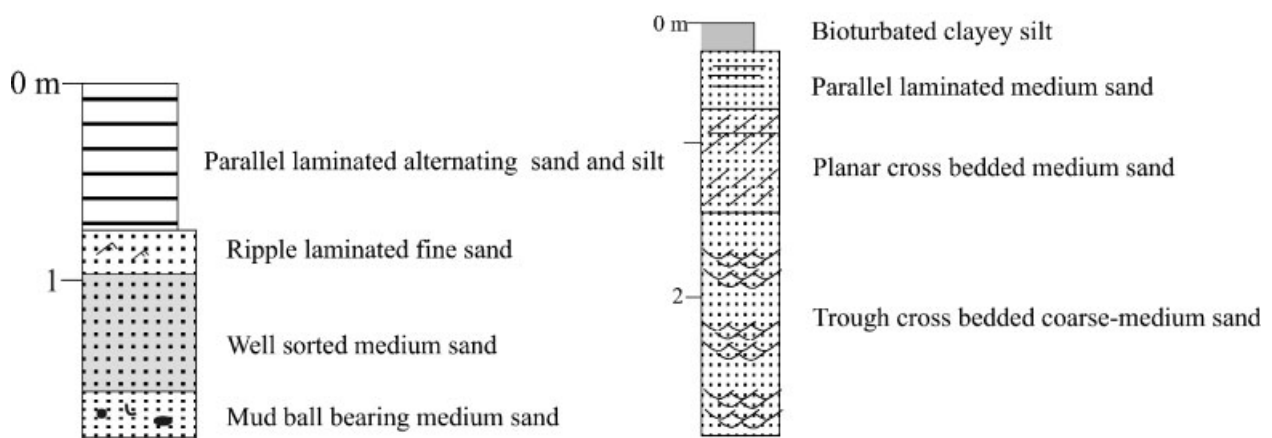


**Figure 5** Schematic diagram showing the lithofacies of Interdune Facies Association and the Channel Facies Association sediments

## Parallel-laminated alternating sand-silt

Units are 0.4–0.7 m thick and consist of couplets of fine sand and silt. Individual couplets are up to 1 cm thick, with the sand layer up to 8 mm thick. Often the silty layers are more clayey and may then be up to 5 cm thick, showing mud cracks and animal footprints (Fig. 6). In places there are bioturbated horizons and some units show several cycles of bioturbated and sand–silt laminations. The direct association with dune sand indicates deposition by sheet flows on dune flanks and in interdune areas. Bioturbated horizons may represent hiatuses in sedimentation. This facies is well developed in the sediments of D-1 and in Sections 2A–2C at Dead Vlei (D-2).

## Trough cross-bedded coarse to medium sand

Units are 1.5–2.2 m thick, moderately well-sorted trough cross-bedded sand. Average grain size is 0.4–0.6 mm and units are rich in coarse lithic fragments. The troughs occur in cossets ca. 80 cm thick, where individual troughs have wavelengths up to 3 m and amplitudes of 50 cm. Laterally the units are lensoid with an erosional basal contact. There is often a pebbly channel lag at the base (Figs 7 and 8a). Trough axes indicate an average palaeocurrent direction of 210°. The facies is well developed in Sections 3A and 3B in D-3.

This lithofacies was deposited by the three-dimensional migration of sand bars under channel flow conditions (Miall, 1996). The grain size and presence of lithic fragments indicate increased erosion and sediment transport in the upper parts of the catchment.

## Planar cross-bedded medium sand

This lithofacies is a red, planar cross-bedded, medium sand 0.3–0.8 m thick (Fig. 7). Sandy pebbles are sometimes present at the base of the unit. The units occur in cossets of cross-bedded sand where individual sets are 5–20 cm thick and generally overly trough cross-bedded medium sand lithofacies. The average palaeocurrent direction is 150°. This facies is well developed in Sections 3A and 3B and was deposited by active mega-ripples (Ashley, 1990).

## Parallel-laminated medium sand

This is 0.3–1.4 m thick parallel-laminated medium sand. Individual laminae are up to 4 mm thick and often show discordances and the occasional presence of mud balls (Fig. 7). The facies overlies trough cross-bedded coarse–medium sand or planar cross-bedded medium sand units and transforms upwards into ripple-laminated sand. It represents sedimentation on a bar during a waning flood (Miall, 1996).

## Bioturbated clayey silt

This is an extensively bioturbated, reddish-brown clayey silt, 0.5–1.0 m thick (Fig. 7). It often occurs in association with ripple-laminated fine sand or parallel-laminated medium sand, forming a gradational contact with the underlying facies. It represents sedimentation in a floodplain setting or bar top sedimentation after the flood recedes (Miall, 1996).

## Lithofacies associations

On the basis of vertical and lateral facies changes, the lithofacies described above can be grouped into two associations (Fig. 5).

## Channel facies associations

These form lensoidal, fining upward sand bodies usually with trough cross-bedded medium sand, overlain by cross-bedded medium sand and parallel-laminated medium sand grading into rippled fine sand near the base. This sequence is overlain by bioturbated clayey silt (Fig. 7). We believe that this association was deposited in a vertically aggrading river valley, where sedimentation was in channel bars and associated floodplains. Channel lag gravels often mark the former position of the stream channel (Fig. 8(B)). Trough-cross-bedding and planar-cross-bedding directions diverge by ca. 60° but indicate an average river palaeoflow of 182° ( $N=15$ ). This facies association is only present in sediments at D-3 (Sections 3A and 3B).

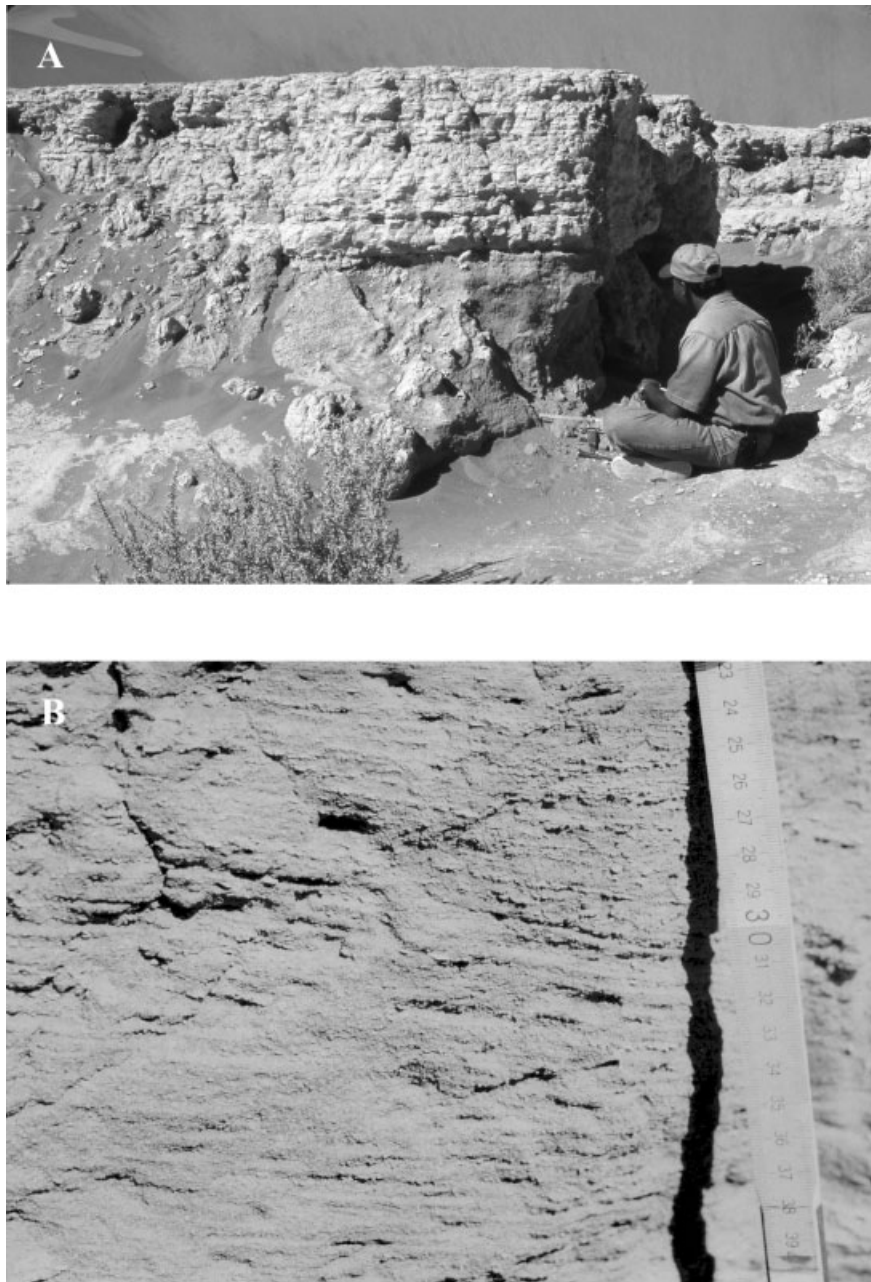


**Figure 6** Sediments of Section 2C in Dead Vlei (A) parallel-laminated sand and silt overlying well-sorted medium dune sand. (B) Alternating parallel-laminated sand and silt lithofacies

We considered the possibility that this association represents a drying ephemeral channel but discounted this interpretation because: (a) the sediments show no features typical of channel desiccation; (b) the bioturbated clay shows a gradational contact with much bioturbation indicating considerable riparian vegetation and animal activity which would be unlikely in a drying channel situation; and (c) there is no dune sand in the sequence as might be expected as a river channel desiccates.

#### Interdune facies associations

These form sheet-like silty, sand units alternating with aeolian dune sand. This facies association includes the following lithofacies: well-sorted medium sand, medium sand with mud balls, ripple-laminated fine sand, and parallel-laminated alternating sand silt. Lensoidal units of ripple-laminated fine sand overlying well-sorted medium sand indicates the formation of small

channels in interdune corridors during high floods in the main channel. The packages of parallel-laminated alternating sand, silt, and dune sand represent sheet flows over dune slopes as water spills from the main stream into interdune areas during high floods (Stanistreet and Stollhofen, 2002). The presence of gravel, mud balls and clay curls in the sandy units is an indication of flood intensity, and the thickness of alternating units of dune sand a measure of the relative intensity of aeolian activity. Bioturbated horizons are a record of plant and animal activity on surfaces wetted by flooding, and they may record hiatuses in flooding.

#### Luminescence dating

Luminescence dating was used to establish a chronology for the interdune and stream channel facies associations (Aitken,

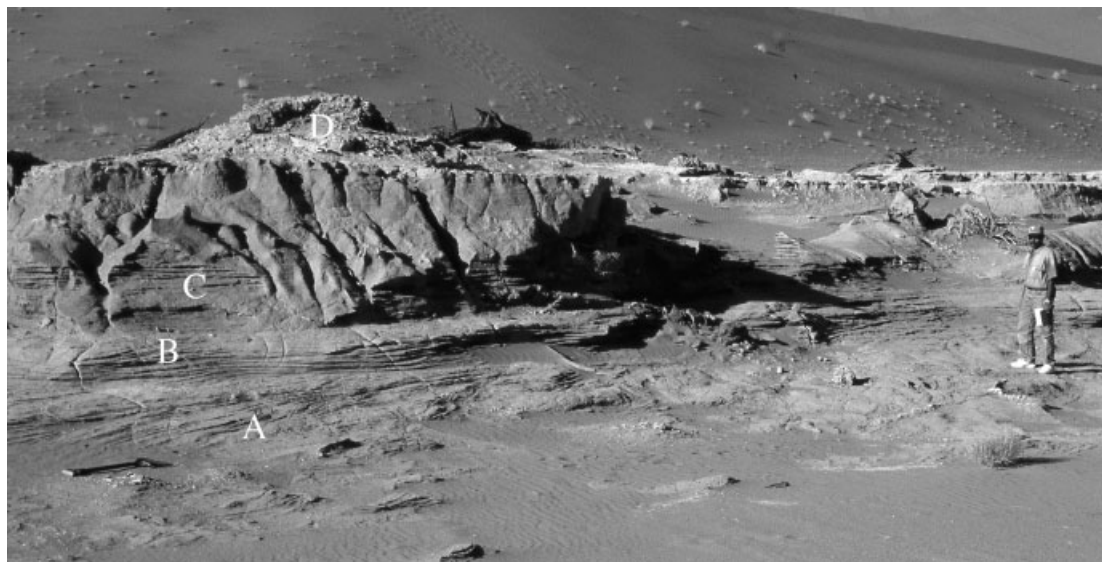


**Figure 7** Channel bar sediments exposed at Section 3A in depression D-3. (A) Trough cross-bedded sand. (B) Planar cross-bedded sand. (C) Parallel-laminated sand. (D) Bioturbated silty clay

1985, 1998). There is increasing evidence that many fluvial sediments are sufficiently well-bleached during transport to make them suitable for OSL dating (Colls *et al.*, 2001; Stokes *et al.*, 2001; Wallinga *et al.*, 2001; Eitel *et al.*, 2002; Heine and Heine, 2002; Bourke *et al.*, 2003; Rittenour *et al.*, 2003; Leigh *et al.*, 2004; Srivastava *et al.*, 2004, 2005). However, OSL single-grain minimum ages (the average of the youngest 10% of grains) are believed to most closely approximate the true ages of sediments (e.g. Roberts *et al.*, 1998, 1999; Wallinga, 2002; Olley *et al.*, 2004). By comparing 9.6-mm and 4-mm single-aliquot minimum ages with single-grain minimum ages for a suite of fluvial sediments from the Kuiseb River, Srivastava *et al.* (2006) found that 4-mm aliquot minimum ages closely approximate single-grain minimum ages. Olley *et al.* (2004) also show that minimum ages of small (10-grain) aliquots provide an accurate estimate of the burial dose for 9 of 12 independently dated, Holocene-age aeolian, fluvial and marine sediments. So, in this study we have used the 4-mm aliquot minimum ages as the best estimates of the ages of our samples.

The lithofacies composition of sediments in the three interdune depressions was analysed and 10 samples were collected from sandy units for luminescence dating (Figs 2–4). To avoid exposure to light, samples were collected by hammering opaque pipes into cleaned, vertical, exposed sections of sediment. Luminescence dating assumes that the geological luminescence of sediment is reduced to near zero by exposure to sunlight during weathering and transport (Aitken, 1985, 1998).

Optically stimulated luminescence (OSL) dating was carried out in subdued red-light conditions. Five centimetres of sediment was removed from each end of the sample pipes for dose rate estimation. Luminescence measurements were made on the central section of the sediment cylinder that was least likely to have been exposed to sunlight during sampling. All samples were treated with 10% HCl and 30% H<sub>2</sub>O<sub>2</sub> to remove carbonates and organic matter. Samples were sieved to extract the 150–170- $\mu$ m-size fraction. Quartz and feldspar grains were separated by density using Na-polytungstate ( $\rho = 2.58 \text{ g cm}^{-3}$ ). The quartz fraction was etched using 40% HF for 80 min followed by 12N HCl for 30 min to remove the skin affected by alpha radiation. The quartz grains were mounted on stainless steel disks using Silkospray<sup>TM</sup>. Light stimulation of the quartz was achieved using a RISØ array of blue LEDs centred at

470 nm. Detection optics comprised Hoya 2  $\times$  U340 and Schott BG-39 filters coupled to an EMI 9635 QA Photomultiplier tube. Measurements were taken with a RISØ TL-DA-15 reader.  $\beta$ -radiation was applied using a 25 mCi <sup>90</sup>Sr/<sup>90</sup>Y in-built source.

The SAR protocol (Murray and Wintle, 2000) was used to determine the palaeodose. A five-point measurement strategy was adopted with three dose points to bracket the palaeodose, a fourth zero dose and a fifth repeat-palaeodose point. The repeat palaeodose was measured to correct for sensitivity changes and check that the protocol was working correctly. All measurements were made at 125 °C for 100 s after a pre-heat to 220 °C for 60 s. For all aliquots the recycling ratio between the first and the fifth point ranged within 0.95 to 1.05. Data were analysed using the ANALYST program of Duller (1999).

For age determination, and as a means of assessing whether the fluvial sediments were totally bleached at deposition, palaeodose measurements were made on single aliquots of 9.6 mm and 4.0 mm diameter. In each case 12–16 aliquots from each sample were analysed. This approach produced two age datasets that could be compared. Dose-rate calculation relied on the thick source ZnS (Ag) alpha counting technique for elemental concentration of uranium and thorium. Potassium was measured by ICP90 using the Sodium Peroxide Fusion technique at the SGS Laboratory in Toronto, Canada. As precipitation over the Tsauchab catchment is in the range 0–175 mm yr<sup>-1</sup> (Jacobson *et al.*, 1995), a water content of 5  $\pm$  2% was assumed for all samples. The cosmic ray gamma contribution was assumed to be 150  $\pm$  30  $\mu$ Gy yr<sup>-1</sup> as recommended for sediments located below an altitude of 1000 m between latitudes 0° and 40° (Prescott and Stephan, 1982).

Radioactivity data are shown in Table 1 and the 9.6-mm and 4.0-mm aliquot age data for the 10 samples analysed, including central and minimum ages, in Table 2 and Fig. 9. If the sediments were totally bleached at deposition we would expect minimum age estimates from both the 9.6-mm and 4.0-mm aliquots to be comparable. However, if the sediments were only partially bleached the 4.0-mm aliquot minimum ages should be younger because the smaller sample size increases the possibility of obtaining a higher percentage of grains that were bleached at deposition. In fact, the 4.0-mm aliquot minimum ages of seven of the 10 samples dated are younger than the

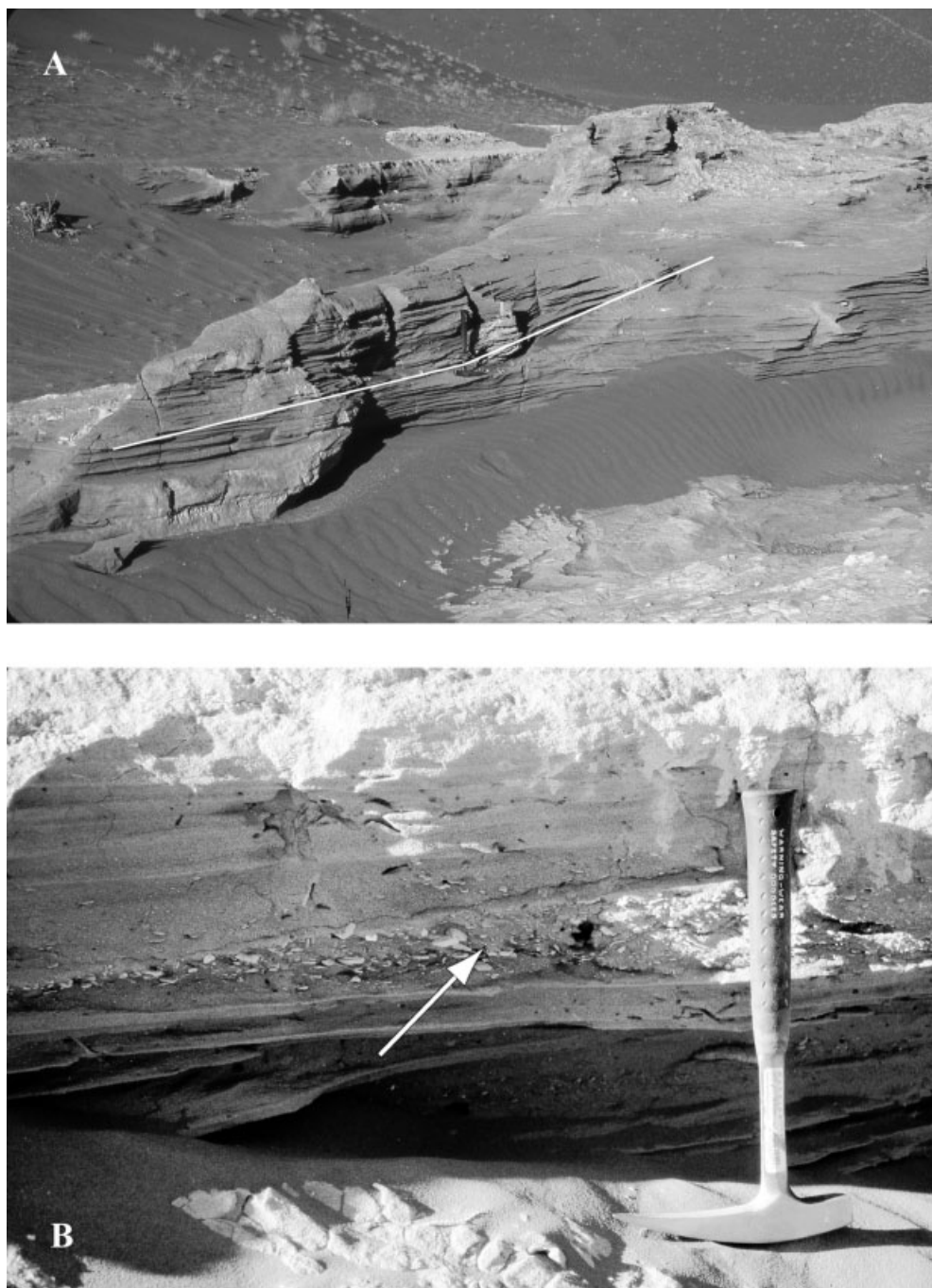


**Figure 8** Sediments of Depression D-3. (A) Trough cross-bedded sand. (B) Pebbly channel lag representing a channel event. The hammer is 40 cm long

**Table 1** Radioactivity data and computed dose rates for the Sossus Vlei samples

Sample No	Sample ID	Depth (m)	U (ppm)	Th (ppm)	K (%)	Dose rate (Gy ka <sup>-1</sup> )
1	SV-1	8.70	1.3 ± 0.2	3.3 ± 0.9	1.74	2.2 ± 0.2
2	SV-2	8.50	1.3 ± 0.3	4.2 ± 1.2	1.73	2.2 ± 0.2
3	SV-5	5.60	1.7 ± 0.3	3.8 ± 1.2	1.65	2.4 ± 0.2
4	SV-6	0.30	1.1 ± 0.2	2.4 ± 0.7	1.60	2.1 ± 0.2
5	DV-1	0.25	1.9 ± 0.3	2.7 ± 1.1	1.24	1.9 ± 0.1
6	DV-2	0.70	2.5 ± 0.3	2.1 ± 1.1	1.20	1.9 ± 0.1
7	DV-3	1.10	1.5 ± 0.3	3.1 ± 1.1	1.43	2.0 ± 0.1
8	DV-4	0.30	1.3 ± 0.3	4.5 ± 1.2	1.36	2.0 ± 0.1
9	DV-5	1.20	1.2 ± 0.2	2.3 ± 0.8	1.49	1.9 ± 0.1
10	DV-6	3.10	1.8 ± 0.8	3.1 ± 1.3	1.53	2.2 ± 0.2

Water content: 5 ± 2% of each sample.

Cosmic ray gamma-radiation: 150 ± 30 μGy ka<sup>-1</sup>.

**Table 2** Luminescence age data for the Sossus Vlei sediments

Sample ID	Dose rate (Gy ka <sup>-1</sup> )	Multiple grain							
		9.6-mm aliquot				4-mm aliquot			
		Central P (Gy)	Minimum P (Gy)	Central Age (ka)	Minimum Age (ka)	Central P (Gy)	Minimum P (Gy)	Central Age (ka)	Minimum Age (ka)
SV-1	2.2±0.2	64.9±6.9	48.4±2.1	29.9±4.4	21.0±1.6	75.8±11.1	56.5±3.5	32.9±5.2	<b>24.6±2.1</b>
SV-2	2.2±0.2	32.0±5.1	29.6±1.8	14.5±2.8	12.6±1.1	34.1±11.0	21.5±2.0	14.5±4.8	<b>9.1±1.0</b>
SV-5	2.4±0.2	32.8±5.9	22.9±1.8	13.9±2.8	9.8±1.0	34.1±8.2	21.6±3.5	14.6±3.7	<b>9.2±1.6</b>
SV-6	2.1±0.2	17.9±2.9	12.4±0.6	8.6±1.6	6.0±0.5	18.4±5.4	8.9±0.8	8.9±2.7	<b>4.3±0.5</b>
DV-1	1.9±0.1	1.5±0.1	1.2±0.1	0.8±0.1	0.6±0.3	1.3±0.5	0.6±0.1	0.7±0.3	<b>0.33±0.06</b>
DV-2	1.9±0.1	3.3±0.7	1.8±0.2	1.7±0.4	0.9±0.1	2.9±1.0	1.7±0.2	1.5±0.5	<b>0.9±0.1</b>
DV-3	2.0±0.1	21.9±3.2	15.0±0.6	10.7±1.7	7.3±0.6	24.0±6.3	11.9±0.5	11.8±3.2	<b>5.8±0.5</b>
DV-4	2.0±0.1	1.7±0.2	1.3±0.1	0.8±0.1	0.6±0.07	1.8±0.2	1.4±0.1	0.9±0.1	<b>0.7±0.07</b>
DV-5	1.9±0.1	4.1±0.9	2.2±0.2	2.1±0.5	1.1±0.1	3.0±1.5	1.2±0.1	1.5±0.8	<b>0.6±0.06</b>
DV-6	2.2±0.2	1.9±0.4	1.1±0.1	0.9±0.2	0.5±0.07	2.1±1.0	0.9±0.1	1.0±0.5	<b>0.4±0.06</b>

9.6-mm aliquot ages by up to 3.5 ka, suggesting partial bleaching of the fluvial sediments. Minimum ages were the same for DV-2 ( $0.9 \pm 0.1$  ka) but 9.6-mm aliquot minimum ages were younger for SV-1 ( $21.0 \pm 1.6$  versus  $24.6 \pm 2.1$  ka) and DV-4 ( $0.6 \pm 0.07$  versus  $0.7 \pm 0.07$  ka). Given this evi-

dence of partial bleaching of our samples (see also Bourke *et al.*, 2003), and the findings of Wallinga (2002), Olley *et al.* (2004) and Srivastava *et al.* (2006), we used the 4-mm single-aliquot minimum ages as the most likely ages of the sediments in the Sossus Vlei area.

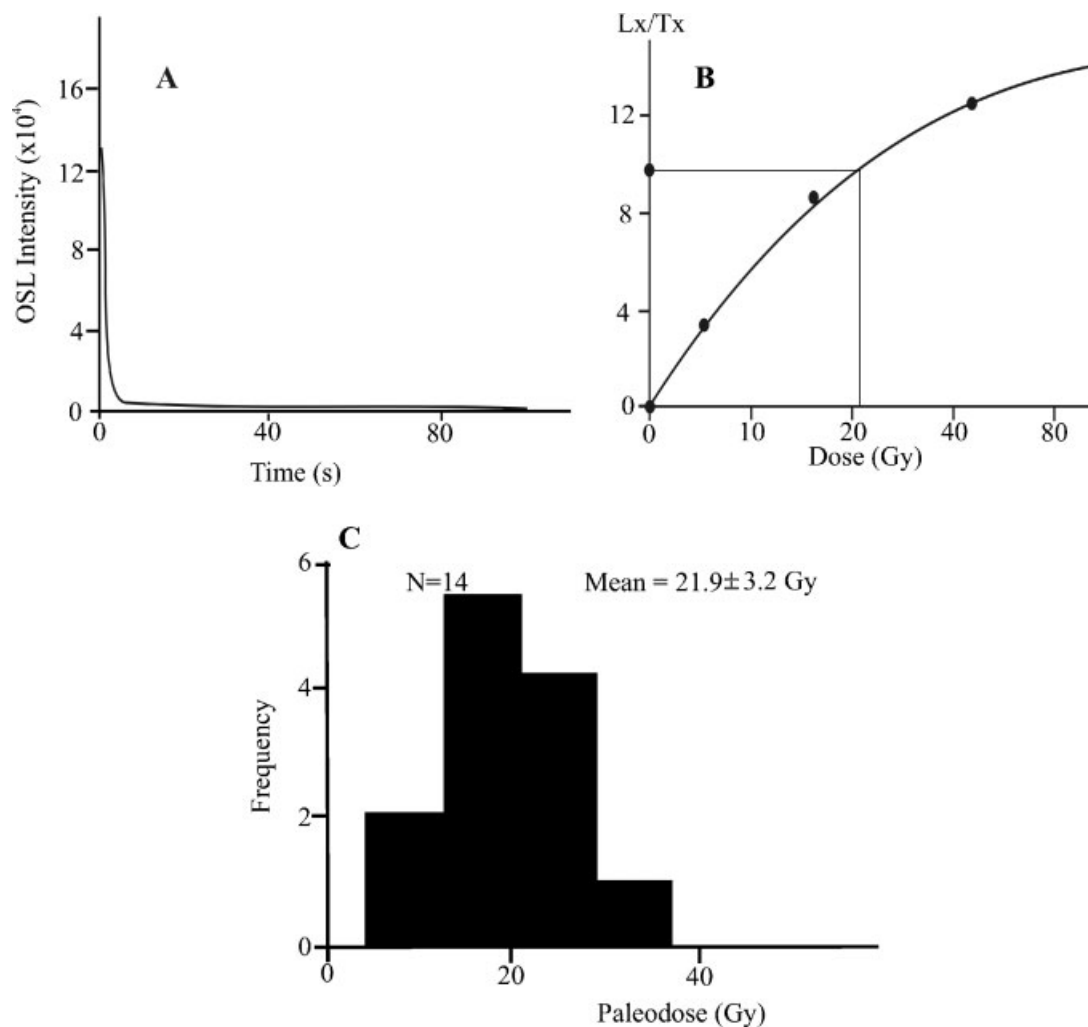


**Figure 9** Single-aliquot (9.6 mm) regeneration data for sample DV-3. (A) OSL shine-down curve against stimulation time. (B) OSL regenerative growth curve against laboratory-induced doses. Lx/Tx is the test dose-corrected ratio of the OSL signal. (C) Frequency distribution of palaeodoses measured on 14 aliquots

## Interpretation and ages of the sedimentary sequences

### Depression 1

The sediments in D-1 consist of a ca. 9 m thick sequence of interdune facies with rounded gravels exposed at the base (Fig. 2). The lower ca. 3.5 m of the sequence shows cycles of medium sand with mud balls and units of parallel-laminated alternating silt–sand without the presence of dune sand. In contrast, the upper ca. 5.5 m of sediment shows parallel-laminated alternating sand–silt facies deposited in association with dune sand. The dune sand increases in thickness upward and there is a parallel decrease in the thickness of the sand–silt facies. This indicates that the basal part of the sequence was deposited at a time of relatively wetter conditions when the river had a higher energy; at least enough to erode clay-silt and carry mud balls into the interdune areas with relatively subdued aeolian activity. Animal footprints on the top of the basal unit also indicate that animals used the area. This suggests that the river extended west of its present position to this depression at this time. During deposition of the upper part of the sequence the dune field extended northwards into the area owing to a gradual decrease in fluvial energy ultimately isolating Depression 1.

The ca. 9 m of sediments in D-1 were deposited from  $24.6 \pm 2.1$  ka (SV-1) to  $4.3 \pm 0.5$  ka (SV-6). However, ages of  $9.2 \pm 1.6$  ka (SV-5) and  $9.1 \pm 0.1$  ka (SV-2) at ca. 5.5 and 8 m respectively indicate that the bulk of deposition occurred from ca. 9–4 ka (Fig. 2). The more fluvial-dominated and possibly wetter part of the sequence shows two discrete episodes of deposition, the first at ca. 24.6 ka and, after a considerable break, the second at ca. 9–7 ka. Before 25 ka the fluvial regime was still well established as indicated by the rounded gravels at the base of the sequence. The overlapping ages in the later episode indicate a short-lived, rapid phase of sedimentation. The upper sediment sequence deposited from 9.2 to 4.3 ka records gradually increasing aridity.

### Depressions 2 and 3

Three sediment sequences, Sections 2A–2C, were examined in D-2. These rest on the dune sand and show primarily the development of the interdune facies association with lensoid rippled sand bodies indicating sedimentation in interdune areas when the flood water escapes during high floods (Fig. 3). The ripple-laminated sand bodies may indicate formation in shallow distributary channels within the interdune areas.

The sedimentary succession in D-3 (Sections 3A and 3B) is made up of the channel facies association and indicates that sedimentation took place exclusively in the form of a channel bar in a southerly flowing river (Fig. 4). Unlike today, the river had a well-developed channel and flood plain. The divergence of ca.  $60^\circ$  in palaeocurrent directions between the two bed forms (troughs and planar cross-beds), suggests that the three-dimensional bedforms (trough cross-bedding) and two-dimensional bedforms (planar cross-bedding) moved in different directions during the evolution of the bar. This may indicate changing current directions and energy of the river because of interference in flow by nearby dunes. However, similar divergence has been reported in the deposits of the perennial River Ganga in the humid tropics of India where it has been considered part of a braid bar sequence (Shukla *et al.*, 1999).

Sedimentation in D-2 and D-3 marks another phase of active fluvial sedimentation when river discharge was high

enough to transport sediments in the form of two- and three-dimensional bedforms forming bars. The interdunal deposits in Dead Vlei (Sections 2A–2C) may indicate flooding of this interdunal area when the Tsauchab River had established a course a little south of its present position, and periodically spilled into neighboring interdune areas. This may have occurred at a time of wetter climate in the catchment and slightly reduced dune activity.

Dune sand at the bases of the Dead Vlei sediment Sections 2A–2C has a luminescence age of  $5.8 \pm 0.5$  ka (DV-3) and the overlying fluvial sediment an age between  $0.9 \pm 0.1$  ka and  $0.3 \pm 0.06$  ka. The D-3 sequences (Sections 3A and 3B) yielded ages between  $0.6 \pm 0.06$  ka and  $0.4 \pm 0.02$  ka. This indicates that the fluvial sedimentation recorded in Sections 2A–C and 3A–B occurred between 0.9 and 0.3 ka and was preceded by more arid conditions from 5.8 to 0.9 ka, based on the age of the underlying dune sand at Dead Vlei.

Calibrated radiocarbon ages for dead *Acacia erioloba* trees in Dead Vlei (D-2) show that the trees started growing by  $770 \pm 33$  cal. yr BP (AD 1180 or 0.8 ka) when the area was presumably wetter than now. The trees died between  $610 \pm 53$  cal. yr BP and  $520 \pm 11$  cal. yr BP (AD 1340–1430 or 0.65–0.6 ka), presumably because of much drier conditions. This record supports sedimentary evidence for frequent flooding of the interdune areas and slightly wetter conditions between 0.9 and 0.3 ka.

The present study of Tsauchab River sediments indicates fluvial sedimentation and wetter conditions at ca. 25 and ca. 9 ka with a minor wet phase between 0.9 and 0.3 ka. Intervening time periods may have been drier or the depressions may have been isolated from the river's influence as a result of dune development.

## Discussion

There is a growing body of evidence from Namibia to indicate discrete periods of wet and dry climate during the last 30 ka. However, at present it is difficult to compare palaeoenvironmental records based on calibrated radiocarbon and U-series ages with those based on OSL ages. One reason for this is that OSL chronologies are usually developed using central ages obtained by analysing large aliquots. Current thinking on OSL dating is that minimum ages determined by single-grain or small-aliquot OSL analyses most closely approximate the true age of the deposit (e.g. Roberts *et al.*, 1999; Wallinga, 2002; Olley *et al.*, 2004; Thomas *et al.*, 2005). We have found that minimum ages determined by the SAR protocol using a 4-mm aliquot closely match calibrated radiocarbon ages and single-grain minimum ages (Srivastava *et al.*, 2006). The decision on whether to use minimum or central OSL ages is significant as minimum ages can be substantially younger than central ages. In this study 9.6-mm aliquot central ages are 0.2–8.9 ka older than minimum ages, the difference generally increasing with increasing sample age, and 4.0-mm aliquot central ages 0.2–8.3 ka older (Table 2).

In Fig. 10 we have assembled some important minimum age OSL, and radiocarbon-dated climate records from the Namib and Kalahari Desert regions and nearby areas that can be compared chronologically with the Sossus data reported here. These include several records based on the ages of secondary carbonates such as spring tufas and pan carbonates in the Namib Desert and adjacent areas (Vogel and Visser, 1981; Lancaster, 1989; Vogel, 1989; Teller *et al.*, 1990), tufas along

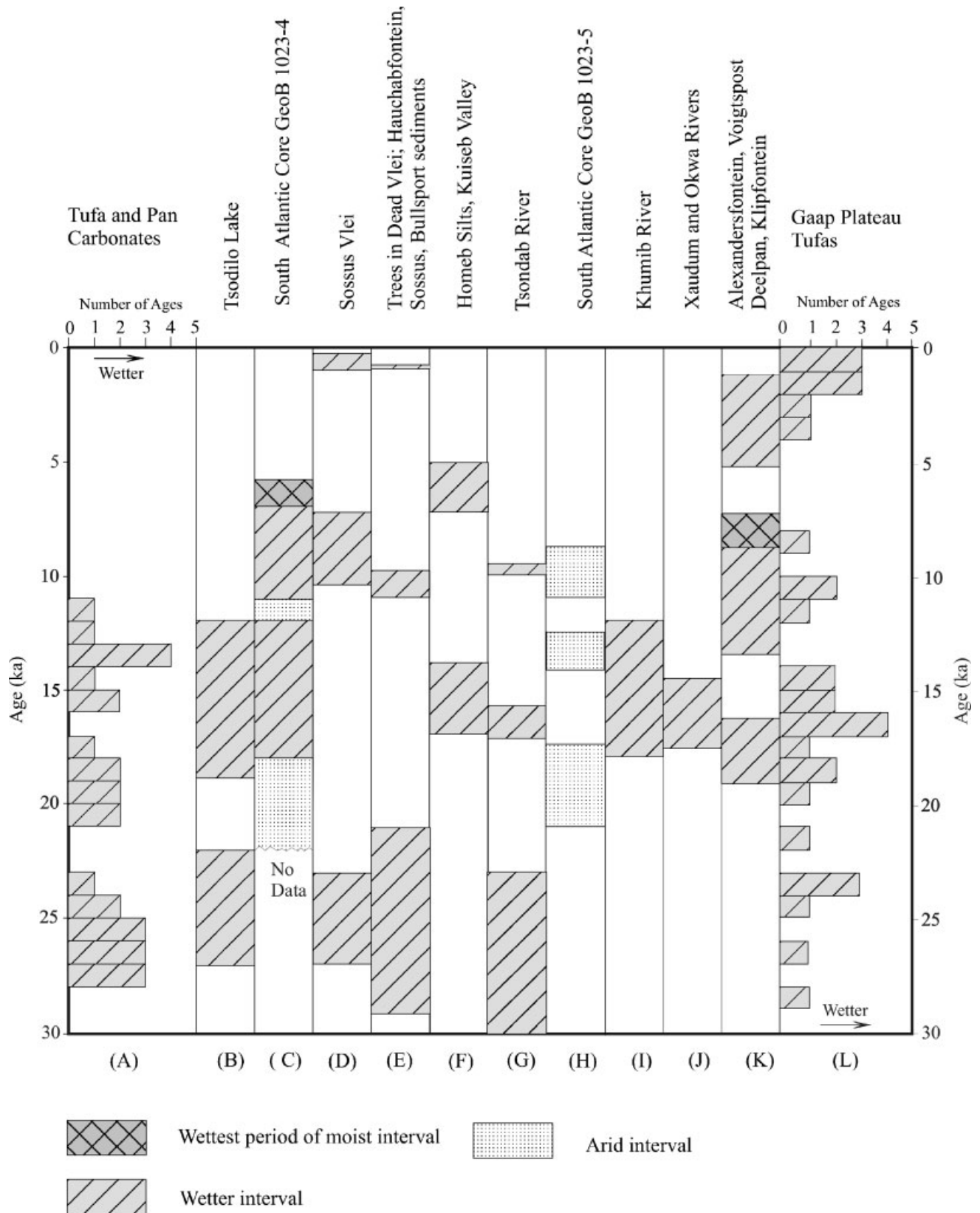


**Figure 10** The Sossus Vlei record compared with other regional palaeoclimate records fixed by calibrated radiocarbon ages. (A) Frequency of tufa and pan carbonate ages in the Namib Desert and nearby areas (Lancaster, 1979; Vogel and Visser, 1981; Rust, 1984; Deacon and Lancaster, 1988; Teller and Lancaster, 1986; Vogel, 1989; Teller *et al.*, 1990; Brook *et al.*, 1999). (B) Lake development at the Tsodilo Hills, NW Botswana (Robbins *et al.*, 2000; Thomas *et al.*, 2003). (C) Summary climate record from the GeoB 1023–4 core indicating maximum wetness at 7–6 ka (Gingele, 1996). (D) The Sossus Vlei record (this paper). (E) Sossus Vlei, Hauchabfontein, and Bullsport sediments (Heine, 1998), and dead trees in Dead Vlei (Vogel, 2003). (F) Deposition of the Homeb silts, Kuiseb valley (Srivastava *et al.*, 2006). (G) Periods of increased flow of the Tsondab River (Vogel and Visser, 1981; Lancaster, 1984; Deacon and Lancaster, 1988). (H) Periods of aeolian activity in South Atlantic marine core GeoB 1023–5 (Shi *et al.*, 2000). (I) Relict fluvial deposits in the Khumib valley (after Srivastava *et al.*, 2004 but with 4-mm aliquot minimum ages used). (J) Increased flow of the Xaudum and Okwa rivers, Botswana (Shaw *et al.*, 1992). (K) Wet intervals in pans at Alexandersfontein, Voigtspost, Deelpan and Klipfontein (Butzer, 1984 a,b; Butzer *et al.*, 1973). (L) Ages of the Gaap Escarpment tufas (Butzer *et al.*, 1978; Beaumont and Vogel, 1993)

the Gaap Escarpment in South Africa (Butzer *et al.*, 1978; Beaumont and Vogel, 1993), and pan carbonates at Alexandersfontein, Voigtspost, Deelpan and Klipfontein in South Africa (Butzer, 1984a,b; Butzer *et al.*, 1973) and at the Tsodilo Hills in NW Botswana, where there is currently no standing water (Robbins *et al.*, 2000; Thomas *et al.*, 2003). Also included are periods of increased fluvial activity in the Tsondab valley 70 km north of Sossus Vlei (Vogel and Visser, 1981; Lancaster, 1984; Deacon and Lancaster, 1988) and in the Xaudum and Okwa valleys of northwestern Botswana (Shaw *et al.*, 1992). Chronologies for these records are based on calibrated radiocarbon ages but no corrections have been made for the possible inclusion of old dead carbon (the hard water effect) as we have no way of knowing the exact amount of such contamination. Vogel (1989) suggests that a correction of about  $-1$  ka is appropriate prior to calibration for tufas and pan carbonates. If correct, this means that ages of secondary carbonates in Fig. 10, columns (A), (B), (E), (G) and (J)–(L), are perhaps ca. 1 ka too old.

Figure 10 also shows the OSL ages of relict fluvial deposits in the Khumib and Kuiseb valleys of Namibia that we believe required increased river flow for their deposition (Srivastava *et al.*, 2004; Srivastava *et al.*, 2006). The Khumib ages are 4-mm aliquot minimum ages rather than the large aliquot central ages listed in Srivastava *et al.* (2004); the Kuiseb chronology is fixed by ages that are averages of single grain minimum ages and 4-mm aliquot minimum ages for each sample analysed. Information from the South Atlantic Ocean coring site GeoB 1023 (cores 4 and 5) is also presented. This site is seaward of the Kunene River mouth and so marine cores provide evidence of wet and arid climate phases in Namibia (Gingele, 1996; Shi *et al.*, 2000).

One very important aspect of Fig. 10 is the good correspondence between the Sossus Vlei, Hauchabfontein and Bullspoor sediment ages (all sites within the Tsauchab River catchment) of Heine (1998) and the ages of dead trees in Dead Vlei (Vogel, 2003), with the OSL ages presented here (columns (D) and (E) in Fig. 10). We believe this agreement between a radiocarbon-based chronology and our OSL chronology is further confirmation that OSL 4-mm aliquot minimum ages very closely approximate the true ages of a deposit.

Despite numerous attempts to synthesise the available data there is still no consensus on climate changes in Namibia during the last 30 ka. For example, Lancaster (2002) suggests that the Namib Desert experienced three wetter periods of climate at 38–31, 28–23, and 14.5–9 ka. Rust and Vogel (1988) identify five periods of increased precipitation in the northern Namib Desert in the last 30 ka at 28–27, 20–19, 13–12, 7–4.5, and 1 ka, and Vogel (1989) three periods at  $>40$ –29, 20–13 and 4.4–1.5 ka.

The palaeoclimate data of Fig. 10 are perhaps the most reliable compilation available. They indicate marked wet intervals of climate at ca. 25, 15, 9–5 and 0.6 ka and there is good agreement between the terrestrial and marine information. There is only partial agreement with the records presented previously by Rust and Vogel (1988), Vogel (1989), and Lancaster (2002). In particular, in Fig. 10, the ages of sediments in the west flowing ephemeral Kuiseb (Homeb silts), Tsondab, Tsauchab and Khumib rivers of Namibia appear to correspond. Also, marine core GeoB 1023–5 arid intervals at 21–17.5, 14.3–12.6, and 11–8.9 ka (Shi *et al.*, 2000) fit fairly well into gaps in the record of moist conditions.  $^{14}\text{C}$  dates for a log preserved in Khumib River sediments near the coast suggest increased discharge at 0.4 ka (Vogel, 1989) while trees buried by fluvial silts in the Amspoort area of the Hoanib valley record wetter conditions at 0.6–0.05 ka followed by a drier climate that led to silt accumulation (Eitel *et al.*, 2005). These young

ages agree with our finding of increased fluvial activity at Sossus Vlei at 0.9–0.3 ka.

Recent studies have shown a strong positive relationship between SE Atlantic sea surface temperatures (SSTs) off Angola and Namibia and rainfall along the coast and inland. A warmer ocean increases the flux of moisture to the Zaire Air Mass thus increasing rainfall along the intertropical convergence zone (ITCZ) as it moves south during the austral summer months. Also, some warm events off the Namibian coast, the so-called 'Benguela-Niños', are preceded by reduced trade winds in the tropical and equatorial Atlantic Ocean (Rouault *et al.*, 2003). These observations raise the possibility that increased rainfall in the past was triggered by weaker South East Trades that led to reduced upwelling of the Benguela Current and therefore to a warmer ocean off the Namibian coast.

Several studies of marine cores off the Angolan and Namibian coasts provide evidence to test this theory. For example, grain-size data and alkenone temperatures from sediment cores MD962086 and MD962087 off Luderitz suggest a negative correlation between increasing wind strength and water temperature, indicating that strong Southeast Trade Winds in the past increased upwelling of the Benguela Current (Pichevin *et al.*, 2005). Periods of low wind strength and warmer water off the Namibian coast during Oxygen Isotope Stages 3, 2 and 1 correlate well with reconstructed positions of the Angola–Benguela front (Jansen *et al.*, 1996) and indicate warmer water off the coast at ca. 24, 15 and 10 ka, at times when there is evidence of increased rainfall inland (Fig. 10).

Little *et al.* (1997) suggest that conditions in the SE Atlantic affected ocean temperatures in the North Atlantic as well as ice sheet conditions. They show that *Neogloboquadrina pachyderma* (s) peaks (PS events) in marine cores GeoB1711 and PG/PC12 off Walvis Bay, that indicate intense upwelling of the cold Benguela Current and strong Southeast Trade Winds, correlate with interstadials in the Greenland GISP 2 ice core isotope record and precede Heinrich events by about 3 ka. They hypothesise that intensification of the trade winds increases cross-equatorial flow and delivers more warm water to the tropical pool for transport northwards. The increase in heat flux from the equator to the high latitudes of the North Atlantic via the Gulf Stream, leads to increased ice accumulation and thermal instabilities that result in rapid ice sheet calving and ultimately ice sheet collapse (Heinrich events).

The most recent PS events were 37–33 (PS3), 29–26 (PS2), and 22–19 ka (PS1) ago, so that increased fluvial activity at Sossus Vlei ca. 25 ka occurred between PS2 and PS1, at a time of reduced upwelling, weaker Southeast Trade Winds, and a warmer southeast Atlantic. Directly supporting increased fluvial activity at this time is aeolian dust and hemipelagic mud largely of fluvial origin in marine core MD962094 from the Walvis Ridge off the northwest coast of Namibia, just south of the Kunene River mouth. The large amount of hemipelagic mud compared to aeolian dust indicates reduced continental aridity ca. 25 ka and increased input of sediments from stream runoff (Stuut *et al.*, 2002).

## Conclusions

Sediments in interdunal depressions D-1 to D-3 near Sossus Vlei lack the carbonate deposits, thick clay beds, and mollusc shells normally associated with river end-point or groundwater seepage deposits. Instead, the channel-related facies and interdune facies associations in the litho-sections indicate

deposition due to increased channel activity and associated flooding of interdune corridors.

The present end-point of the Tsauchab River is at Sossus Vlei. Relict fluvial sediments 2–3 km W and SW of this end-point indicate vigorous fluvial activity further into the Namib Sand Sea ca. 25 and 9 ka and then later at ca. 0.9–0.3 ka. Regional data suggest an additional wet interval at ca. 15 ka that has so far not been identified in the Sossus Vlei area. Our OSL 4-mm aliquot minimum ages for sediments near Sossus correspond well with calibrated radiocarbon ages suggesting they closely match the true ages of the deposits, raising the possibility that published OSL ages determined by using mean ages of large aliquots may be too old.

The deposits discussed here give only a minimal range for the western extent of fluvial activity because they represent channel sediments. Associated end-point deposits of the Tsauchab River must lie deeper into the Namib Sand Sea in, or under, the dunes.

Further work is needed west of Sossus Vlei to determine whether there was increased fluvial activity ca. 15 ka, as the regional record suggests, and to more fully document the flooding history of the Tsauchab and its former penetration into the Namib Sand Sea. These data will help assess the rate of migration of Namib sand dunes into this area and the changing balance between moving sand and fluvial activity.

*Acknowledgements* The research was funded by NSF grant BCS-0002193 and was conducted under permits issued by the National Monuments Council and the Ministry of Environment and Tourism of Namibia. We thank Nicholas Lancaster and David Thomas who provided helpful suggestions on the manuscript.

## References

- Aitken MJ. 1985. *Thermoluminescence Dating*. Academic Press: London.
- Aitken MJ. 1998. *An Introduction to Optical Dating*. Academic Press: London.
- Ashley GM. 1990. Classification of large-scale subaqueous bedforms: a new look at an old problem. *Journal of Sedimentary Petrology* **60**: 160–172.
- Beaumont PB, Vogel JC. 1993. What turned the young tufas on at Gorrokop? *South African Journal of Science* **89**: 196–198.
- Bourke MC, Child A, Stokes S. 2003. Optical age estimates for hyper-arid fluvial deposits at Homeb, Namibia. *Quaternary Science Reviews* **22**: 1099–1103.
- Brook GA, Marais E, Cowart JB. 1999. Evidence of wetter and drier conditions in Namibia from tufas and submerged speleothems. *Cimbebasia* **15**: 29–39.
- Butzer KW. 1984a. Late Quaternary environments in South Africa. In *Late Cainozoic Palaeoclimates of the Southern Hemisphere*, Vogel JC (ed.). A.A. Balkema: Rotterdam; 235–264.
- Butzer KW. 1984b. Archaeogeology and Quaternary environment in the interior of southern Africa. In *Southern African Prehistory and Palaeoenvironments*, Klein RG (ed.). A.A. Balkema: Rotterdam; 1–64.
- Butzer KW, Fock GJ, Stuckenrath R, Zilch A. 1973. Paleohydrology of late Pleistocene Lake Alexandersfontein, Kimberley, South Africa. *Nature* **243**: 328–340.
- Butzer KW, Stuckenrath R, Bruzewicz AJ, Helgren DM. 1978. Late Cenozoic paleoclimates of the Gaap Escarpment, Kalahari margin, South Africa. *Quaternary Research* **10**: 310–339.
- Colls AE, Stokes S, Blum MD, Straffin E. 2001. Age limits on the late Quaternary evolution of the upper Loire River. *Quaternary Science Reviews* **20**: 743–750.
- Deacon J, Lancaster N. 1988. *Late Quaternary Environments of Southern Africa*. Oxford University Press: Oxford.
- Duller GAT. 1999. Luminescence Analyst computer programme V2.18. Department of Geography and Environmental Sciences, University of Wales, Aberystwyth.
- Eitel B, Blümel WD, Hüser K. 2002. Environmental transition between 22 ka and 8 ka in monsoonally influenced Namibia—a preliminary chronology. *Zeitschrift für Geomorphologie* **126**: 31–57.
- Eitel B, Kadereit A, Blümel WD, Hüser K, Kromer B. 2005. The Amspoort silts, northern Namib Desert (Namibia): formation, age and palaeoclimatic evidence of river-end deposits. *Geomorphology* **64**: 299–314.
- Gingeles FX. 1996. Holocene climatic optimum in Southwest Africa—evidence from the marine clay mineral record. *Palaeogeography, Palaeoclimatology, Palaeoecology* **122**: 77–87.
- Heine K. 1993. Zum alter jungquartärer Feuchtphasen im ariden und semiariden südwestlichen Afrika. *Würzburger Geographische Arbeiten* **87**: 149–162.
- Heine K. 1998. Climate change over the past 135,000 years in the Namib Desert (Namibia) derived from proxy data. *Palaeoecology of Africa* **25**: 171–198.
- Heine K, Heine JT. 2002. A paleohydrologic reinterpretation of Homeb Silts, Kuiseb River, central Namib Desert (Namibia) and paleoclimatic implications. *Catena* **48**: 107–130.
- Jacobson PJ, Jacobson KM, Seely MK. 1995. *Ephemeral Rivers and their Catchments: Sustaining People and Development in Western Namibia*. Desert Research Foundation of Namibia: Windhoek.
- Jansen JHF, Ufkes E, Schneider, RR. 1996. Late Quaternary movements of the Angola-Benguela Front, SE Atlantic, and implications for advection in the equatorial ocean. In *The South Atlantic: Present and Past Circulation*, Wefer G, Berger WH, Siedler G, Webb DJ (eds). Springer: Berlin; 553–575.
- Krapf CEB, Stollhofen H, Stanistreet IG. 2003. Contrasting styles of ephemeral river systems and their interaction with dunes of Skeleton Coast Erg (Namibia). *Quaternary International* **104**: 41–52.
- Lancaster N. 1979. Evidence for a widespread late Pleistocene humid period in the Kalahari. *Nature* **279**: 145–146.
- Lancaster N. 1982. Dunes of Skeleton Coast, Namibia (South West Africa): geomorphology and grain size relationships. *Earth Surface Processes and Landforms* **7**: 575–587.
- Lancaster N. 1984. Palaeoenvironments of the Tsondab valley, central Namib Desert. *Palaeoecology of Africa* **16**: 411–419.
- Lancaster N. 1989. Late Quaternary palaeoenvironments in the southwestern Kalahari. *Palaeogeography, Palaeoclimatology, Palaeoecology* **70**: 367–376.
- Lancaster N. 2002. How dry was dry? Late Pleistocene palaeoclimates in the Namib Desert. *Quaternary Science Reviews* **21**: 769–782.
- Lancaster N, Teller JT. 1988. Interdune deposits of the Namib sand sea. *Sedimentary Geology* **55**: 91–107.
- Leigh DS, Srivastava P, Brook GA. 2004. Late Pleistocene braided rivers on the Atlantic Coastal Plain, U.S.A. *Quaternary Science Reviews* **23**: 65–84.
- Little MG, Schneider RR, Kroon D, Price B, Summerhayes CP, Segl M. 1997. Trade wind forcing of upwelling, seasonality, and Heinrich events as a response to sub-Milankovitch climate variability. *Paleoceanography* **12**: 568–576.
- Miall AD. 1996. *The Geology of Fluvial Deposits*. Springer: Berlin.
- Murray AS, Wintle AG. 2000. Luminescence dating of quartz using improved single-aliquot regenerative-dose protocol. *Radiation Measurement* **32**: 57–73.
- Olley JM, Pietsch T, Roberts RG. 2004. Optical dating of Holocene sediments from a variety of geomorphic settings using single grains of quartz. *Geomorphology* **60**: 337–358.
- Pichevin L, Cremer M, Giraudeau J, Bertrand P. 2005. A 190 ky record of lithogenic grain-size on the Namibian slope: forging a tight link between past wind-strength and coastal upwelling dynamics. *Marine Geology* **218**: 81–96.
- Prescott JR, Stephan LG. 1982. Contribution of cosmic radiation to environmental dose. *PACT (Strasbourg)* **6**: 17–25.
- Rittenour TM, Goble RJ, Blum MD. 2003. An optical age chronology of Late Pleistocene fluvial deposits in the northern lower Mississippi valley. *Quaternary Science Reviews* **22**: 1105–1110.
- Robbins LH, Murphy ML, Brook GA, Ivester AH, Campbell AC, Klein RG, Milo RG, Stewart KM, Downey WS, Stevens NJ. 2000. Archaeology, palaeoenvironment, and chronology of the Tsodilo Hills

- White Paintings Rock Shelter, northwest Kalahari Desert, Botswana. *Journal of Archaeological Science* **27**: 1085–1113.
- Roberts R, Bird M, Olley J, Galbraith R, Lawson E, Laslett G, Yoshida H, Jones R, Fullagar R, Jacobsen G, Hua Q. 1998. Optical and radiocarbon dating at Jinmium rock shelter in northern Australia. *Nature* **393**: 358–362.
- Roberts RG, Galbraith RF, Olley JM, Yoshida H, Laslett GM. 1999. Optical dating of single and multiple grains of quartz from Jinmium rock shelter, northern Australia: Part II, Results and implications. *Archaeometry* **41**: 365–395.
- Rouault M, Reason CJ, Lujeharms JRE, Mulenga H, Richard, Y, Faucher-eau N, Trzaska S. 2003. *Role of the oceans in South Africa's rainfall*. Water Research Commission, Report no. 953/1/03, Gezina, South Africa.
- Rust U. 1984. Geomorphic evidence of Quaternary environmental changes in Etosha, South West Africa/Namibia. In *Late Cainozoic Palaeoclimates of the Southern Hemisphere*, Vogel JC (ed.). A.A. Balkema: Rotterdam; 279–286.
- Rust U, Vogel JC. 1988. Late Quaternary environmental changes in the northern Namib Desert as evidenced by fluvial landforms. *Palaeoecology of Africa* **19**: 127–137.
- Shaw PA, Thomas DSG, Nash J. 1992. Late Quaternary fluvial activity in the dry valleys (mekgacha) of the Middle and Southern Kalahari, southern Africa. *Journal of Quaternary Science* **7**: 273–281.
- Shi N, Dupont LM, Beug H-J, Schneider R. 2000. Correlation between vegetation in southwestern Africa and oceanic upwelling in the past 21,000 years. *Quaternary Research* **54**: 72–80.
- Shukla UK, Singh IB, Srivastava P, Singh DS. 1999. Paleocurrent patterns in braid-bar and point-bar deposits: examples from the Ganga River, India. *Journal of Sedimentary Research* **69**: 992–1002.
- Srivastava P, Brook GA, Marais E. 2004. A record of fluvial aggradation in the northern Namib Desert during the Late Quaternary. *Zeitschrift für Geomorphologie N.F.* (Suppl.-Vol.) **133**: 1–18.
- Srivastava P, Brook GA, Marais E. 2005. Depositional environment and luminescence chronology of the Hoarusib River Clay Castles sediments, northern Namib Desert, Namibia. *Catena* **59**: 187–204.
- Srivastava P, Brook GA, Marais E, Morthekai P, Singhvi AK. 2006. Depositional environment and single aliquot and single grain OSL chronology of the Homeb Silt Deposits, Kuiseb River, Namibia. *Quaternary Research* in press.
- Stanistreet IG, Stollhofen H. 2002. Hoanib River flood deposits of Namib Desert interdunes as analogues for thin permeability barrier mudstone layers in aeolianite reservoirs. *Sedimentology* **49**: 719–736.
- Stokes S, Thomas DSG, Washington R. 1997. Multiple episodes of aridity in southern Africa since the last interglacial period. *Nature* **388**: 154–158.
- Stokes S, Bray HE, Blum MD. 2001. Optical resetting in large drainage basins: tests of zeroing assumptions using single-aliquot procedures. *Quaternary Science Reviews* **20**: 879–885.
- Stuut J-BW, Prins MA, Schneider RR, Weltje GJ, Jansen JHF, Postma G. 2002. A 300-kyr record of aridity and wind strength in southwestern Africa; inferences from grain-size distributions of sediments on Walvis Ridge, SE Atlantic. *Marine Geology* **180**: 221–233.
- Svendsen J, Stollhofen H, Krapf CBE, Stanistreet IG. 2002. Mass and hyperconcentrated flow deposits record dune damming and catastrophic breakthrough of ephemeral rivers, Skeleton Coast Erg, Namibia. *Sedimentary Geology* **160**: 7–31.
- Teller JT, Lancaster N. 1986. Lacustrine sediments at Narabeb in the central Namib Desert, Namibia. *Palaeogeography, Palaeoclimatology, Palaeoecology* **56**: 177–195.
- Teller JT, Rutter NW, Lancaster N. 1990. Sedimentology and palaeohydrology of late Quaternary lake deposits in the northern Namib Sand Sea, Namibia. *Quaternary Science Reviews* **9**: 343–364.
- Thomas DSG, Shaw PA. 2002. Late Quaternary environmental change in central southern Africa: new data, synthesis, issues and prospects. *Quaternary Science Reviews* **21**: 783–797.
- Thomas DSG, Brook GA, Shaw P, Bateman M, Haberyan K, Appleton C, Nash D, McLaren S, Davies F. 2003. Late Pleistocene wetting and drying in the NW Kalahari: an integrated study from the Tsodilo Hills, Botswana. *Quaternary International* **104**: 53–67.
- Thomas PJ, Jain M, Juyal N, Singhvi AK. 2005. Comparison of single grain and small aliquot OSL dose estimates in <3000 years old river sediments from south India. *Radiation Measurement* **39**: 457–469.
- Vogel JC. 1989. Evidence of past climatic change in the Namib Desert. *Palaeogeography, Palaeoclimatology, Palaeoecology* **70**: 355–366.
- Vogel JC. 2003. The age of dead trees at Sossus and Tsondab Vleis, Namib Desert, Namibia. *Cimbebasia* **18**: 247–251.
- Vogel JC, Visser E. 1981. Pretoria radiocarbon dates II. *Radiocarbon* **23**: 43–80.
- Wallinga J. 2002. Optically stimulated luminescence dating of fluvial deposits: a review. *Boreas* **31**: 303–322.
- Wallinga J, Duller GAT, Murray AS, Törnqvist TE. 2001. Testing optically stimulated luminescence dating of sand-sized quartz and feldspar from fluvial deposits. *Earth and Planetary Science Letters* **193**: 617–630.
- Ward JD. 1987. *The Cenozoic succession in the Kuiseb Valley, Central Namib Desert*. Geological Survey of Namibia, Memoir 9; 124.